

## Impact of Deposition Temperature on Indium Trioxide's Structural and Optical Properties

Reem M. Khalafa<sup>a</sup>, Makram A. Fakhri<sup>b,\*</sup>, Zaid T. Salim<sup>c</sup>, Motahher A. Qaeed<sup>d</sup>, A. Mindil<sup>d</sup>, Subash C. B. Gopinath<sup>e, f, g</sup>, Ahmed A. Al-Amiery<sup>h</sup>

<sup>a</sup>Al-Farahidi University, Baghdad, Iraq

<sup>b</sup>College of Laser and Optoelectronic Engineering, University of Technology-Iraq, Baghdad, Iraq

<sup>c</sup>College of Energy and Environmental Sciences, Al-Karkh University of Science, Baghdad 10081, Iraq

<sup>d</sup>Department of Physical Sciences, Faculty of Science, University of Jeddah, Jeddah, Saudi Arabia

<sup>e</sup>Center for Global Health Research, Saveetha Medical College & Hospital Saveetha Institute of Medical and Technical Sciences (SIMATS), Thandalam, Chennai – 602 105, Tamil Nadu, India

<sup>f</sup>Faculty of Chemical Engineering & Technology and Institute of Nano Electronic Engineering, Universiti Malaysia Perlis (UniMAP), 02600 Arau, Perlis, Malaysia

<sup>g</sup>Department of Technical Sciences, Western Caspian University, Baku AZ 1075, Azerbaijan. 5Al-Mustaqbal University College, Department of Medical Physics, Iraq

<sup>h</sup>Al-Ayen Scientific Research Center, Al-Ayen Iraqi University, AUIQ, P.O. Box: 64004, An Nasiriyah, Thi Qar, Iraq

\*Corresponding author. Tel.: +964y7702793869; e-mail: Makram.a.fakhri@uotechnology.edu.iq, mokaram\_76@yahoo.com

### ABSTRACT

This study examined how altering the deposition temperature affected the characteristics of the indium oxide thin (In<sub>2</sub>O<sub>3</sub>) films that were produced. using silicon bases and the pulsed laser deposition (PLD) technique. In<sub>2</sub>O<sub>3</sub> films (nanoparticles) were prepared by the PLD method utilizing a 1064 nm wavelength (Nd:YAG) laser. Atomic force microscopy, UV-visible spectroscopy, Field Emission Scanning Electron Microscopy (FE-SEM), and x-ray diffraction (XRD) were used to describe the sample. The films' polycrystalline structure was demonstrated by the X-ray diffraction pattern data. image of a microscope Atomic force microscopy (AFM) analysis showed that the films made using the PLD process had a homogenous surface, and UV-visible spectroscopy revealed that spherical nanoparticles with altered optical characteristics emerge when the temperature of deposition changes. The produced films' absorbance, transmittance, and energy gap spectra, which were examined in relation to their optical characteristics, were 3.91 eV at 300 C.

**Keywords:** Indium Trioxides, Nanostructure, Laser fluencies, PLD, FESEM

### 1. INTRODUCTION

Materials made of semiconductor metal oxide (SMO) make good choices for a variety of electrical devices [1-3]. Their exceptional stability, homogeneity, great transparency, and superior electrical performance have garnered significant attention [4, 5]. studied a great deal. Because of these important features, a wide variety of manufacturing processes are now available that use SMO [6, 7]. For semiconductor gas sensors, the genesis of semiconductivity in metal oxides was investigated for the most significant oxides, such as SnO<sub>2</sub>, In<sub>2</sub>O<sub>3</sub>, ITO, ZnO, Cr<sub>2</sub>O<sub>3</sub>, CuO, and others [8-12]. Their distinct set of functional characteristics—most notably electrical conductivity, transparency throughout a broad spectrum, and strong surface reactivity—place them in the category of transparent conductive oxides [13-16].

Indium oxide, or In<sub>2</sub>O<sub>3</sub>, has recently caught the interest of scientists. In optoelectronic applications, it is a crucial transparent conducting material [17-19]. The material is popularly known as Indium Tin Oxide (ITO) [20, 21], The quintessential Transparent Conducting Oxide (TCO), when doped with SnO<sub>2</sub> [22-24]. Because of its intriguing physical and chemical properties, In<sub>2</sub>O<sub>3</sub> finds extensive use in a variety of technical applications, such as transparent films

for organic light-emitting diodes (OLEDs) and organic photovoltaic cells (OPVC). It is also employed in chemical gas sensing and heterogeneous catalysis. There is ongoing debate over even fundamental material properties as the fundamental band gap [25-28].

An n-type semiconductor is In<sub>2</sub>O<sub>3</sub> [29, 30]. The strong non-stoichiometry seen in highly reducing circumstances is also explained by the intrinsic donor faults that give rise to the n-type conduction. Up until now, In<sub>2</sub>O<sub>3</sub>'s high carrier concentration made it a very good conductor even in the absence of external dopants. Due to its high stability, strong conductivity, and an energy level that is suitable for water splitting, In<sub>2</sub>O<sub>3</sub> may be used in photoelectrochemical (PEC) applications [31-36].

This study used a variety of substrate temperatures and the pulsed laser approach to create thin films. Optimizing In<sub>2</sub>O<sub>3</sub> thin film deposition and examining the resulting films' structural, optical, and morphological characteristics as well as the relationship between these characteristics and deposition parameters like power and working pressure were the main goals of this work.

## 2. EXPERIMENTAL

As seen in Figure 1, which displays the PLD method utilized in this investigation, In<sub>2</sub>O<sub>3</sub> thin films were created on a silicon substrate using the PLD approach. Nd:YAG laser with frequency (3 Hz) and wavelength ( $\lambda = 1.064$  nm). The parameters were displayed accurately. For every 200, 250, 300, 350, and 400 degrees Celsius, China supplied an undoped indium oxide target with 300 pulses. The laser intensity was 800 Mj, and the target was set at a 45-degree angle. Every movie was made with a background oxygen

pressure of 100 mbar. This technique was used to deposit samples onto silicon substrate, as seen in Figure 1. Figure 2 displayed the PLD system's schmtic diagram. The substrate layer was heated to 300 C using a hotplate. The procedures took less than ten minutes to complete. Using a stylus profile meter, the film thickness was determined to be between 71 and 243 nm. The sample of indium oxide thin film nanoparticles (in<sub>2</sub>O<sub>3</sub>) was examined using the FESEM, AFM, U-visible, and XRD tests. The results and debates section that follows provides an analysis of every result.



**Figure 1.** PLD system.

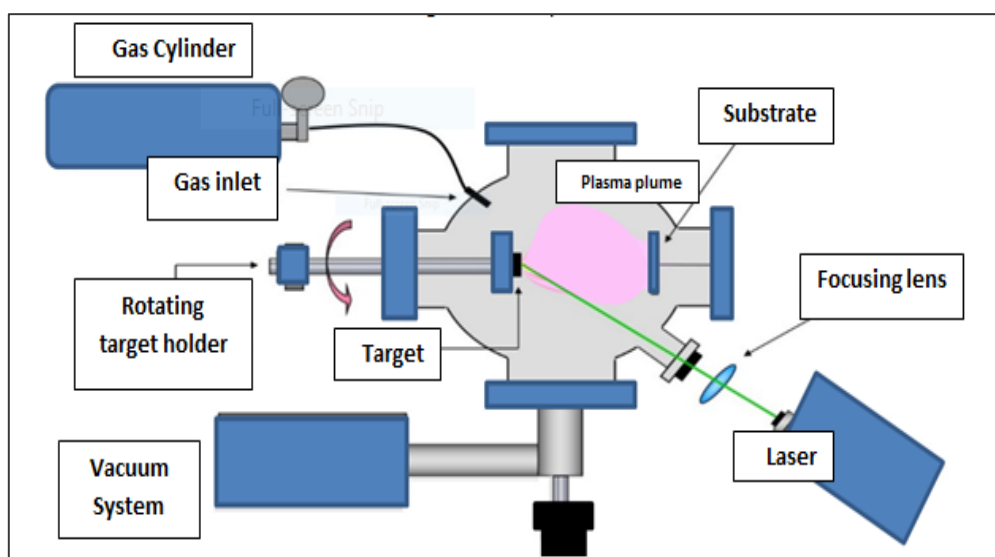


**Figure 2.** The schematic diagram of PLD system.

### 3. RESULTS AND DISCUSSION

#### 3.1. Structural Properties

Figure 3 displayed XRD of the produced thin layer of In<sub>2</sub>O<sub>3</sub> samples. The diffraction peaks at 2 $\theta$  of 30.82°, 35.52°, 51.44°, and 60.79°, reflected from (222), (400), (440), and (622) planes of cubic crystals of In<sub>2</sub>O<sub>3</sub>, respectively [37-39]. It is clear that the heights of the main peaks of the indium(III) oxide nanostructures increase with the increase in the temperature of the pulsed laser deposition substrate,

this increase is attributed to the enhanced cohesion process of the nanocrystals that were ablated using the laser. Therefore, the crystallization process will be enhanced and improved with an increase in the temperature of the deposition substrate. The samples demonstrate that raising the temperature from 200 to 400° C increased the crystalline size [40-43]. A high degree of improvement in the structural properties was also observed, such as the improvement in crystal size, and all XRD data are shown in Table 1.

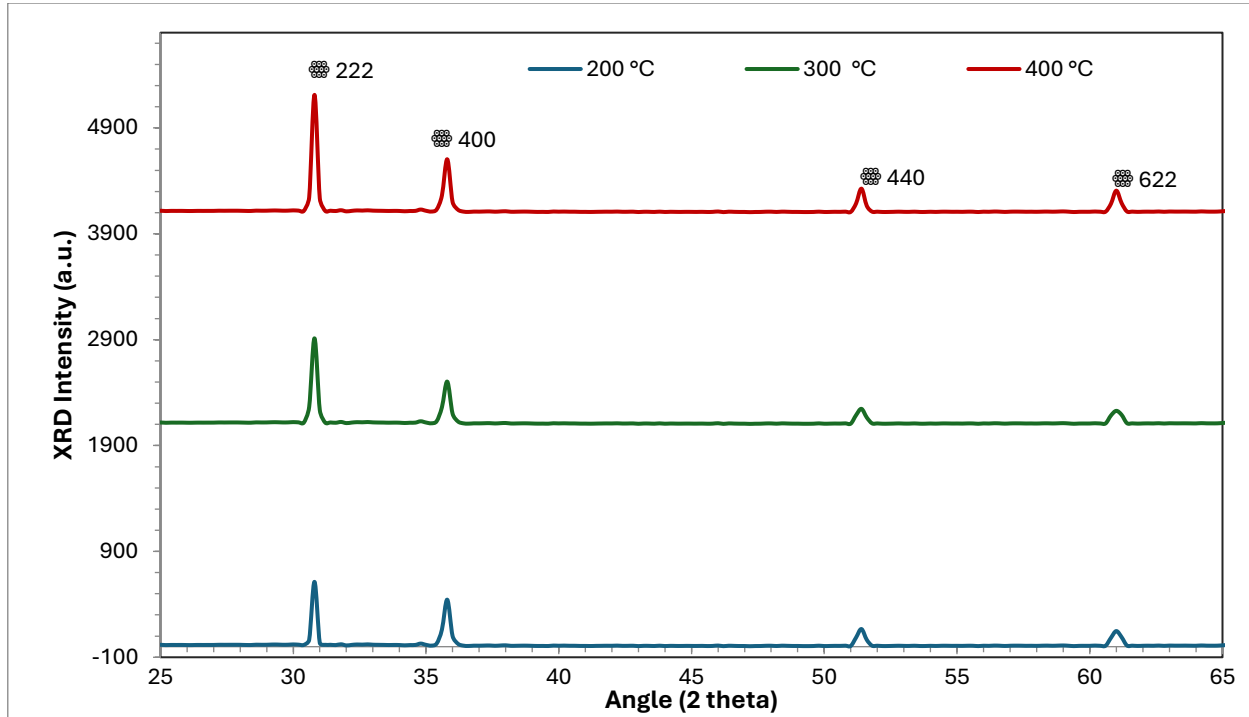


**Figure 3.** XRD spectra at deposition temperature (200-250-300-350-400C).

**Table 1** In<sub>2</sub>O<sub>3</sub> thin-film XRD characteristics at various temperatures (200–250–300–350–400C)

| T   | 2theta | $\beta$ =FWHM(deg) | $D \text{ (nm)} = 0.9\lambda / \beta \cos\theta$ | $d_{\text{spacing}} = \lambda / 2\sin\theta$ | h | k | l | a(A)  |
|-----|--------|--------------------|--|--|---|---|---|-------|
| 200 | 30.8   | 0.4                | 21.52  | 0.28   | 2 | 2 | 2 | 0.969 |
| 200 | 35.8   | 0.22               | 37.97098   | 0.24   | 4 | 0 | 0 | 0.96  |
| 200 | 51.4   | 0.2                | 23.03  | 0.17   | 4 | 4 | 0 | 0.96  |
| 200 | 61.1   | 0.3                | 24.10  | 0.14   | 6 | 2 | 2 | 0.96  |
| 300 | 30.8   | 0.3                | 22   | 0.28   | 2 | 2 | 2 | 0.96  |
| 300 | 35.8   | 0.4                | 12.27  | 0.24   | 4 | 0 | 0 | 0.96  |
| 300 | 51.4   | 0.36               | 22.5   | 0.17   | 4 | 4 | 0 | 0.96  |
| 300 | 61.5   | 0.41               | 27   | 0.98   | 6 | 2 | 2 | 0.96  |
| 400 | 30.8   | 0.2                | 22.5   | 0.28   | 2 | 2 | 2 | 0.96  |
| 400 | 35.8   | 0.23               | 45   | 0.24   | 4 | 0 | 0 | 0.96  |
| 400 | 51.4   | 0.28               | 45   | 0.17   | 4 | 4 | 0 | 0.96  |
| 400 | 61.1   | 0.28               | 32.95  | 0.14   | 6 | 2 | 2 | 0.96  |

3.2. Morphological Properties

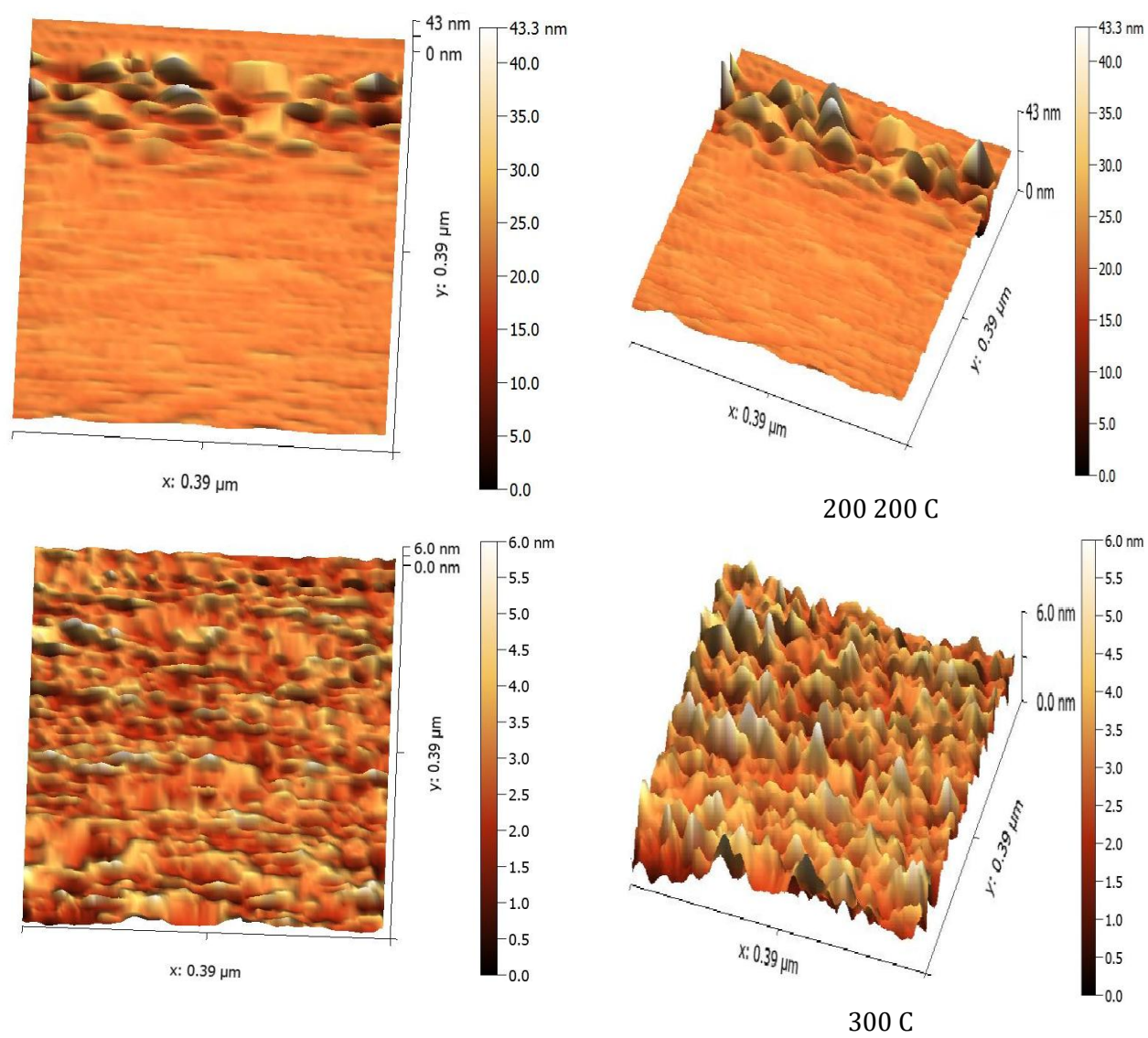
3.2.1. AFM Results

In order to study the topography of the surfaces of the prepared thin films and the extent to which a change in the deposition temperature affects them,(with the ability to image and analyze these surfaces and give very accurate important information about the values of the square root of a square, Roughness Average-Ra).

Two-dimensional atomic force microscope images show In2O3 samples prepared on Silicon floors at different deposition temperatures. The result of changing the

temperature on the dimensions and geometric shape of the prepared samples most clearly manifested in the images of a microscope Atomic forces in Figure 4 [44, 45]. The images also show a increase in the RMS and Ra values of the prepared thin films by increasing the deposition temperature. Values of (RMS) and (Ra) for prepared samples are listed in Table 2 [46, 47].

Figure 4 illustrates how additional grains form as the substrate temperature rises. As the substrate temperature increases, an improvement in grain size can be seen. This finding is consistent with XRD data showing that particle size rises as substrate temperature rises [48-50].





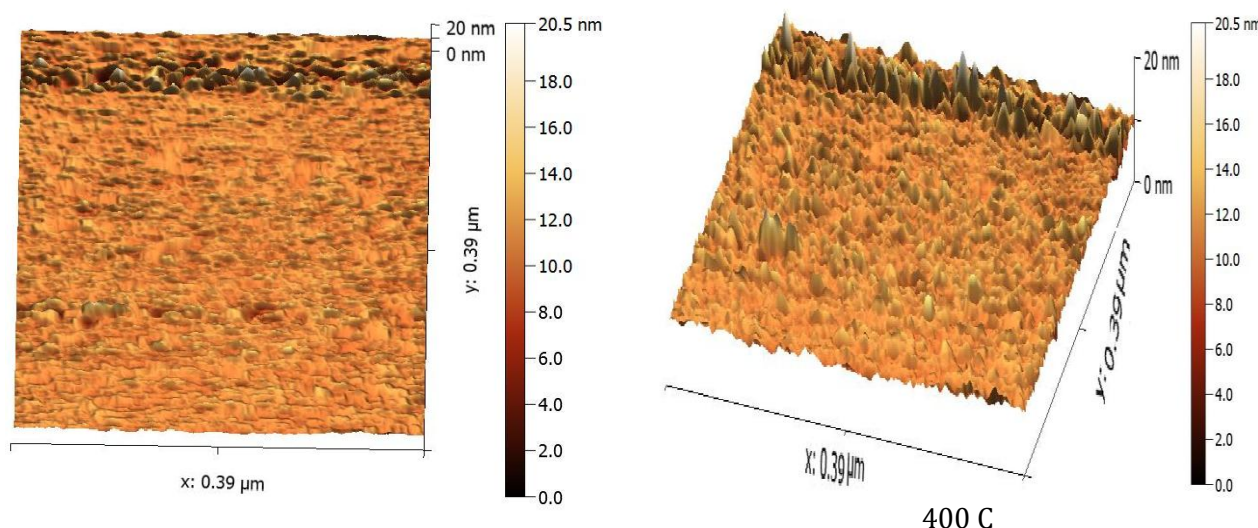


**Figure 4.** Pure In<sub>2</sub>O<sub>3</sub> thin-film AFM pictures at various temperatures (200, 300, and 400 C).

**Table 2** Values of (RMS) and (Ra) for prepared samples

| Sample No. | Temperature (C) | Average roughness (nm) | RMS (nm) | Grain size (nm) |
|------------|-----------------|------------------------|----------|-----------------|
| 1          | 200             | 21.73                  | 2.15     | 93.99           |
| 2          | 300             | 3.37                   | 4.64     | 39.71           |
| 3          | 400             | 11.50                  | 1.36     | 111.27          |

### 3.3. Optical Properties

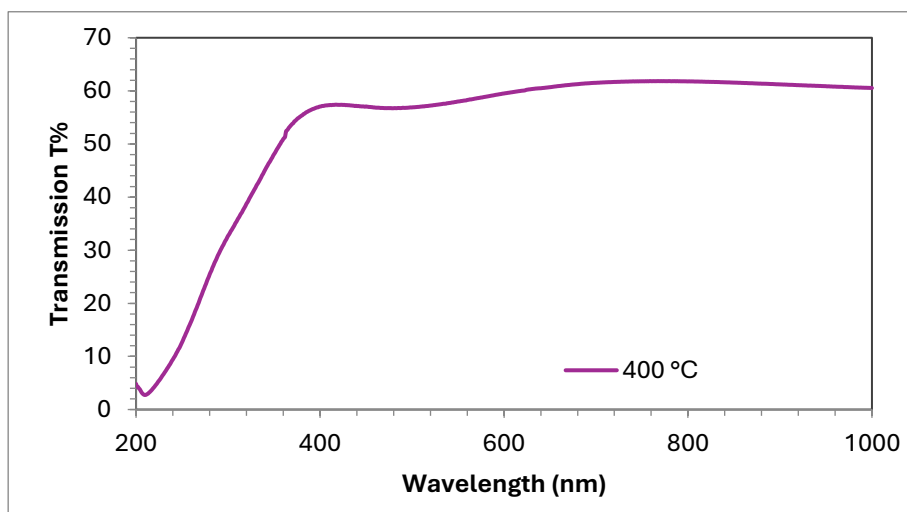
The optical absorbance and transmittance spectra for In<sub>2</sub>O<sub>3</sub> thin films made utilizing a pulsed laser deposition process at optimum substrate temperatures 400 degrees Celsius) are displayed in Figs. 5(a) and 5(b). In this instance, it was discovered that In<sub>2</sub>O<sub>3</sub> thin films had a pronounced absorption edge at wavelengths over 350 nm and were transparent, which is higher than 80%, in the visible range (400–800). As seen in Fig. 6(b), the Nano-thin films have very low absorption in the visible and near-infrared (NIR) region, beginning at 400 nm to 800 nm, but considerable absorption in the UV range [51–54].

The Tauc relation [55–58] has been used to calculate the band gap (E<sub>g</sub>);

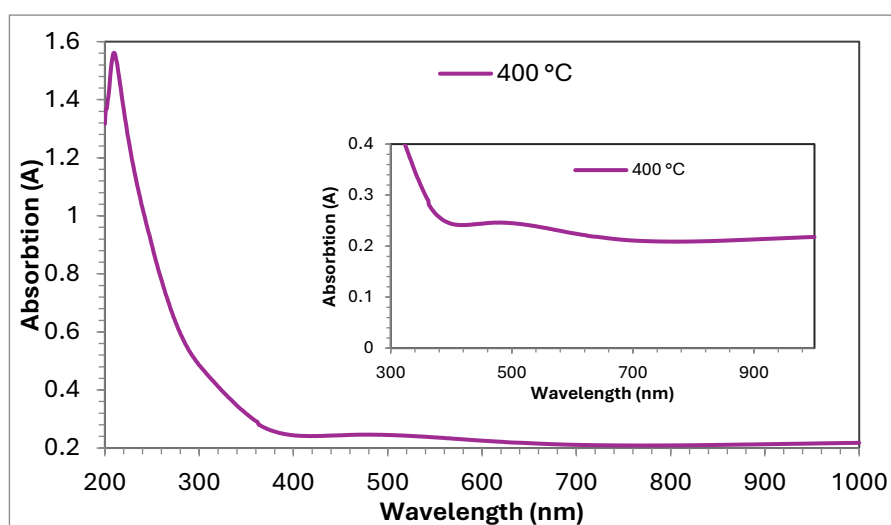
$$(\alpha h\nu)^m = A h\nu - E_g$$

The energy band gap values at optimum deposition temperatures are tabulated in Table 3, where  $h\nu$  is the photon energy,  $A$  is a constant,  $E_g$  is the band gap energy, and  $m$  have values 1/2, 3/2, 2, and 3 depending on the type of electronic transition causing the absorption.

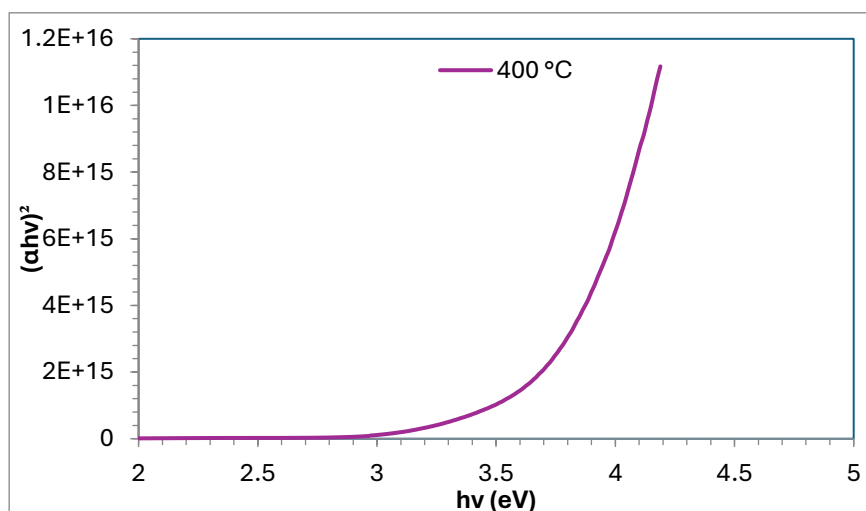
To determine the samples' band gap, Figure 5.c plots  $(\alpha h\nu)^2$  against photon energy ( $h\nu$ ). Plotting the linear part of the plot against the photon energy axis yields the absorption edge, which indicates that the sample has a direct band gap. The In<sub>2</sub>O<sub>3</sub> nanostructure is discovered to have a straight band gap in the 3.53–3.91 eV region [59–63].



(a)



(b)



(c)

**Figure 5.** a) In<sub>2</sub>O<sub>3</sub> Transmittance at optimum deposition temperature (400 °C), b) In<sub>2</sub>O<sub>3</sub> Absorbance at optimum deposition temperature (400 °C). c) In<sub>2</sub>O<sub>3</sub> Energy band gap at optimum deposition temperature.

**Table 3** In2O3 nanostructure Energy band gap at different deposition temperature

| Sample no. | Temperature °C | Energy band gap (eV) |
|------------|----------------|----------------------|
| 5          | 400            | 3.68                 |

#### 4. CONCLUSION

In conclusion, the PLD approach successfully created an In2O3 nanostructured thin film. Indium oxide thin film (In2O3) nanostructure fabrication at five distinct temperatures is presented in this article. XRD, AFM, FESEM, and U-visible investigations were used to examine the In2O3 that was placed on the silicon substrate. The XRD spectrum demonstrates the crystalline cubic structure of the In2O3 nanospheres. At 400 °C, the In2O3 thin films crystallized the best. According to AFM analysis, the average grain size is between 40 and 190 nm. The UV-Vis spectrum (3.91 eV) was used to compute the assessed optical band gap energy. In2O3 nanoparticles are a good material for synthesis gas sensors and optoelectronic device applications because of their strong band gap value.

#### REFERENCE

- [1] Girtan, M., Cachet, H., & Rusu, G. I. (2003). On the physical properties of indium oxide thin films deposited by pyrosol in comparison with films deposited by pneumatic spray pyrolysis. 427, 406–410.
- [2] Prathap, P., Devi, G. G., Subbaiah, Y. P. V., Ramakrishna Reddy, K. T., & Ganesan, V. (2008). Growth and characterization of indium oxide films. *Current Applied Physics*, 8(2), 120–127. <https://doi.org/10.1016/j.cap.2007.06.001>.
- [3] Mohammed, M. M., Rasidi, M., Mohammed, A. M., Rahman, R. B., Osman, A. F., Adam, T., ... & Dahham, O. S. (2022). Interfacial bonding mechanisms of natural fibre-matrix composites: an overview. *BioResources*, 17(4), 7031.
- [4] Wang, B., Zheng, Z., Wu, H., & Zhu, L. (2014). Field emission properties and growth mechanism of In2O3 nanostructures. *Nanoscale Research Letters*, 9(1), 1–8. <https://doi.org/10.1186/1556-276X-9-111>.
- [5] Alakrach, A. M., Noriman, N. Z., Dahham, O. S., Hamzah, R., Alsaadi, M. A., Shayfull, Z., & Syed Idrus, S. Z. (2018, June). The Effects of Tensile Properties of PLA/HNTs-ZrO2Bionanocomposites. In *Journal of Physics: Conference Series* (Vol. 1019, p. 012066). IOP Publishing.
- [6] Dahham, O. S., & Zulkepli, N. N. (2020). Robust interface on ENR-50/TiO2 nanohybrid material based sol-gel technique: insights into synthesis, characterization and applications in optical. *Arabian Journal of Chemistry*, 13(8), 6568-6579.
- [7] Dahham, O. S., Noriman, N. Z., Sam, S. T., Rosniza, H., Marwa, N. A. S., Shayfull, Z., & Alakrach, A. M. (2016). The effects of trans-polyoctylene rubber (TOR) as a compatibilizer on the properties of epoxidized natural rubber/recycled silicone catheter (ENR-25/rSC) Vulcanizate. In *MATEC Web of Conferences* (Vol. 78, p. 01076). EDP Sciences.
- [8] X. P. Shen, H. J. Liu, X. Fan, Y. Yuan, J. M. Hong, and Z. Xu, "Construction and photoluminescence of In2O3 nanotube array by CVD-template method," *J. Crys. Growth* 276, 471-477 (2005).
- [9] Mohammed, M., Rozyanty, R., Mohammed, A. M., Osman, A. F., Adam, T., Dahham, O. S., ... & Betar, B. O. (2018). Fabrication and characterization of zinc oxide nanoparticle-treated kenaf polymer composites for weather resistance based on a solar UV radiation. *BioResources*, 13(3), 6480-6496.
- [10] Stefan Preussler; Hassanain Al-Taiy; Thomas Schneider, Optical spectrum analysis with kHz resolution based on polarization pulling and local oscillator assisted Brillouin scattering, 2015 European Conference on Optical Communication (ECOC), <https://doi.org/10.1109/ECOC.2015.7341758>.
- [11] Stefan Preussler; Hassanain Al-Taiy; Thomas Schneider, Optical spectrum analysis with kHz resolution based on polarization pulling and local oscillator assisted Brillouin scattering, <https://ieeexplore.ieee.org/xpl/conhome/7318283/proceeding>, <https://doi.org/10.1109/ECOC.2015.7341758>.
- [12] L. Dai, X. L. Chen, J. K. Jian, M. He, T. Zhou, and B. Q. Hu, "Fabrication and characterization of In2O3 nanowires," *Appl. Phys. A* 75, 687-689 (2002).
- [13] Stefan Preussler, Hassanain Al-Taiy, and Thomas Schneider, Generation and Stabilization of THz-waves with Extraordinary Low Line Width and Phase Noise, CLEO: 2015, OSA Technical Digest (online) (Optica Publishing Group, 2015),paper STu4H.6, [https://doi.org/10.1364/CLEO\\_SI.2015.STu4H.6](https://doi.org/10.1364/CLEO_SI.2015.STu4H.6).
- [14] Salim, E.T., Fakhri, M.A., Tariq, S.M. et al. The Unclad Single-Mode Fiber-Optic Sensor Simulation for Localized Surface Plasmon Resonance Sensing Based on Silver Nanoparticles Embedded Coating. *Plasmonics* 19, 131–143 (2024). <https://doi.org/10.1007/s11468-023-01949-z>.
- [15] Hassanain Al-Taiy; Thomas Schneider, Drastically SBS Gain Enhancement in Silicon-on-Insulator based Nano-Waveguides, 2013 ITG Symposium Proceedings - Photonic Networks, 2013, 1 – 7.
- [16] M. J. Zheng, L. D. Zhang, G. H. Li, X. Y. Zhang, and X. F. Wang, "Ordered indium-oxide nanowire arrays and their photoluminescence properties," *Appl. Phys. Lett.* 79, 839-841 (2001).

- [17] Ismail R.A.; Salim E.T.; Halbos H.T., Preparation of Nb2O5 nanoflakes by hydrothermal route for photodetection applications: The role of deposition time, *Optik*, 245, 167778 (2021) 10.1016/j.ijleo.2021.167778.
- [18] Mohammed, M.K.A., Naji, A.M., Ahmed, D.S. *et al.* Facile synthesis of chitosan-MoS<sub>2</sub> over reduced graphene oxide to improve photocatalytic degradation of methylene blue. *J Sol-Gel Sci Technol* (2024). <https://doi.org/10.1007/s10971-024-06619-y>.
- [19] Alwazny M.S.; Ismail R.A.; Salim E.T., Aggregation threshold for Novel Au – LiNbO<sub>3</sub> core/shell Nano composite: effect of laser ablation energy fluence, *International Journal of Nanoelectronics and Materials*, 15(3), 223-232 (2022).
- [20] P. Guha, S. Kar, and S. Chaudhuri, "Direct synthesis of single crystalline In<sub>2</sub>O<sub>3</sub> nanopillars and nanocolumns and their photoluminescence properties," *Appl. Phys. Lett.* 85, 3851-3853 (2004).
- [21] Salim E.T.; Halboos H.T., Synthesis and physical properties of Ag doped niobium pentoxide thin films for Ag-Nb<sub>2</sub>O<sub>5</sub>/Si heterojunction device, *Materials Research Express*, 6(6), 66401 (2019) 10.1088/2053-1591/ab07d3.
- [22] Fakhri M.A.; Wahid M.H.A.; Kadhim S.M.; Badr B.A.; Salim E.T.; Hashim U.; Salim Z.T., The structure and optical properties of Lithium Niobate grown on quartz for photonics application, *EPJ Web of Conferences*, 162, 1005 (2017) 10.1051/epjconf/201716201005.
- [23] Roaa A. Abbas, Evan T. Salim & Rana O. Mahdi, Morphology transformation of Cu<sub>2</sub>O thin film: different environmental temperatures employing chemical method, *J Mater Sci: Mater Electron* 35, 1057 (2024). <https://doi.org/10.1007/s10854-024-12823-x>.
- [24] Q. Tang, W. Zhou, W. Zhang, S. Ou, K. Jiang, W. Yu, and Y. Qian, "Size-controllable growth of single crystal In(OH)<sub>3</sub> and In<sub>2</sub>O<sub>3</sub> nanocubes," *Cryst. Growth & Des.* 5, 147-150 (2005).
- [25] Evan T. Salim, Roaa A. Abbas, Raed K. Ibrahim, Rana O. Mahdi, Makram A. Fakhri, Ahmad S. Azzahrani, Forat H. Alsultany, Subash C. B. Gopinath & Zaid T. Salim, Impact of Decoration Method on Some Physical Properties of Ag@Cu<sub>2</sub>O Nanostructure, *Plasmonics* (2024). <https://doi.org/10.1007/s11468-024-02569-x>.
- [26] Alsultany F.H.; Alhasan S.F.H.; Salim E.T., Seed Layer-Assisted Chemical Bath Deposition of Cu<sub>2</sub>O Nanoparticles on ITO-Coated Glass Substrates with Tunable Morphology, Crystallinity, and Optical Properties, *Journal of Inorganic and Organometallic Polymers and Materials*, 31(9), 3749-3759 (2021) 10.1007/s10904-021-02016-y.
- [27] Doaa A. Mahmoud, Evan T. Salim, Rana O. Mahdi, A. Mindil, Subash C. B. Gopinath & Motahher A. Qaeed, Laser Ablation of Tungsten Metal for Au@WO<sub>3</sub> Core-Shell Formation: A Characterizing Study at Different Laser Fluences, *Plasmonics* (2024). <https://doi.org/10.1007/s11468-024-02607-8>.
- [28] Mihaela Gîrtan, G.I. Rusu , *Analele Stiintifice Ale Universitatii "Al.I.Cuza" Din Iasi Tomul Xlv-Xlvi, s. Fizica St ării Condensate*, 1999 . 2000, p. 166 . 172.
- [29] Fakhri M.A.; Al-Douri Y.; Bouhemadou A.; Ameri M., Structural and Optical Properties of Nanophotonic LiNbO<sub>3</sub> under Stirrer Time Effect, *Journal of Optical Communications*, 39(3), 297-306 (2018) 10.1515/joc-2016-0159.
- [30] Khawla S khashan, Rana O Mahdi, Ban A. Badr, Farah Mahdi, Preparation and characterization of ZnMgO nanostructured materials as a photodetector, *Journal of Physics: Conference Series* 1795 (2021) 012008. doi:10.1088/1742-6596/1795/1/012008.
- [31] Fakhri M.A.; Salim E.T.; Wahid M.H.A.; Hashim U.; Salim Z.T., Optical investigations and optical constant of nano lithium niobate deposited by spray pyrolysis technique with injection of Li<sub>2</sub>CO<sub>3</sub> and Nb<sub>2</sub>O<sub>5</sub> as raw materials, *Journal of Materials Science: Materials in Electronics*, 29(11), 9200-9208 (2018) 10.1007/s10854-018-8948-9.
- [32] Mailis, S., Boutsikaris, L., Vainos, N.A., et al., 1996, *Appl. Phys. Lett.*, 69, 2459.
- [33] Salim E.T.; Saimon J.A.; Abood M.K.; Fakhri M.A., Some physical properties of Nb<sub>2</sub>O<sub>5</sub> thin films prepared using nobic acid based colloidal suspension at room temperature, *Materials Research Express*, 4(10), 106407 (2017) 10.1088/2053-1591/aa90a6.
- [34] Fakhri M.A.; Numan N.H.; Mohammed Q.Q.; Abdulla M.S.; Hassan O.S.; Abduljabar S.A.; Ahmed A.A., Responsivity and response time of nano silver oxide on silicon heterojunction detector, *International Journal of Nanoelectronics and Materials*, 11(Special Issue BOND21), 109-114 (2018).
- [35] Roaa A. Abbas, Evan T. Salim, and Rana O. Mahdi, Study based on micro-and nanosized raw materials using the hydrothermal method, *International Journal of Nanoelectronics and Materials (IJNeaM)* Volume 18, No. 1, January 2025 [141-149]. <https://doi.org/10.58915/ijneam.v18i1.1751>.
- [36] K K Makhija, Arabinda Ray†, R M Patel†, U B Trivedi and H N Kapse, *Bull. Mater. Sci.*, Vol. 28, No. 1, February 2005, pp. 9–17. © Indian Academy of Sciences.
- [37] Aseel A. Hadi, Juhaina M. Taha, Rana O. Mahdi, Khawla S. Khashan, Influence of laser pulse on properties of NiO NPs prepared by laser ablation in liquid, *AIP Conf. Proc.* 2213, 020308 (2020) <https://doi.org/10.1063/5.0000115>.
- [38] Evan T. Salim, Ahmed T. Hassan, Rana O Mahdi, Forat H. Alsultany, Physical Properties of HfO<sub>2</sub> Nano Structures Deposited using PLD, *IJNeaM*, vol. 16, no. 3, pp. 495–510, Oct. 2023.
- [39] Fakhri M.A.; Wahid M.H.A.; Badr B.A.; Kadhim S.M.; Salim E.T.; Hashim U.; Salim Z.T., Enhancement of Lithium Niobate nanophotonic structures via spin-coating technique for optical waveguides application, *EPJ Web of Conferences*, 162, 1004 (2017) 10.1051/epjconf/201716201004.
- [40] Xiang Yang Konga,b, Zhong Lin Wang , *Solid State Communications* 128 (2003).



- [41] Evan T. Salim, Rana O. Mahdi, Tamara E. Abdulrahman, Makram A. Fakhri, Jehan A. Siamon, Ahmad S. Azzahrani & Subash C.B. Gopinath, RE-crystallization of Nb<sub>2</sub>O<sub>5</sub> nanocrystals: a study employing different laser wavelength, *J Opt* (2024). <https://doi.org/10.1007/s12596-024-01942-7>.
- [42] Roaa A. Abbas, Evan T. Salim & Rana O. Mahdi, Deposition time effect on copper oxide nano structures, an analysis study using chemical method, *J Mater Sci: Mater Electron* 35, 427 (2024). <https://doi.org/10.1007/s10854-024-12143-0>.
- [43] Fakhri M.A.; Salim E.T.; Wahid M.H.A.; Hashim U.; Salim Z.T.; Ismail R.A., Synthesis and characterization of nanostructured LiNbO<sub>3</sub> films with variation of stirring duration, *Journal of Materials Science: Materials in Electronics*, 28(16), 11813-11822 (2017) [10.1007/s10854-017-6989-0](https://doi.org/10.1007/s10854-017-6989-0).
- [44] C. Grivas, D.S. Gill, S. Mailis, L. Boutsikaris, N.A. Vainos, *Appl. Phys. A* 66, 201-204 (1998).
- [45] Zainab T. Hussain, Khawla S. Khashan, Rana O. Mahdi, Characterization of cadmium oxide nanoparticles prepared through Nd:YAG laser ablation process, *Materials Today: Proceedings* Volume 42, Pages 2645 - 2648 2021. <https://doi.org/10.1016/j.matpr.2020.12.594>.
- [46] Jurn Y.N.; Malek F.; Mahmood S.A.; Liu W.-W.; Gbashi E.K.; Fakhri M.A., Important parameters analysis of the single-walled carbon nanotubes composite materials, *ARPN Journal of Engineering and Applied Sciences*, 11(8), 5108-5113 (2016).
- [47] Hassan M.A.M.; Al-Kadhemy M.F.H.; Salem E.T., Effect irradiation time of Gamma ray on MSISM (Au/SnO<sub>2</sub>/SiO<sub>2</sub>/Si/Al) devices using theoretical modeling, *International Journal of Nanoelectronics and Materials*, 8(2), 69-82 (2015).
- [48] Salih, M.M., Investigation of the effect of electromagnetic radiation on human health using remote sensing technique, *International Journal of Safety and Security Engineering* This link is disabled., 2021, 11(1), pp. 117-122.
- [49] Rana O. Mahdi, Aseel A. Hadi, Juhaina M. Taha, Khawla S. Khashan, Preparation of nickel oxide nanoparticles prepared by laser ablation in water, *AIP Conf. Proc.* 2213, 020309 (2020) <https://doi.org/10.1063/5.0000116>.
- [50] Salim Z.T.; Hashim U.; Arshad M.K.M.; Fakhri M.A., Simulation, fabrication and validation of surface acoustic wave layered sensor based on ZnO/IDT/128° YX LiNbO<sub>3</sub>, *International Journal of Applied Engineering Research*, 11(15), 8785-8790 (2016).
- [51] Ismail R.A.; Salim E.T.; Hamoudi W.K., Characterization of nanostructured hydroxyapatite prepared by Nd:YAG laser deposition, *Materials Science and Engineering C*, 33(1), 47-52 (2013) [10.1016/j.msec.2012.08.002](https://doi.org/10.1016/j.msec.2012.08.002).
- [52] Hashim, A.H., Jasim, O.Z., Salih, M.M., The Establishing of Geospatial Database for Agricultural Lands of Islamic WAQF in Iraq: Case Study Babil Province, *IOP Conference Series: Earth and Environmental Science* This link is disabled., 2022, 961(1), 012025.
- [53] Azzam Y. Kudhur, Evan T. Salim, Ilker Kara, Makram A. Fakhri & Rana O. Mahdi, Structural optical and morphological properties of copper oxide nanoparticles ablated using pulsed laser ablation in liquid, *J Opt* 53, 1936-1945 (2024). <https://doi.org/10.1007/s12596-023-01331-6>.
- [54] Fakhri M.A.; Al-Douri Y.; Hashim U., Fabricated Optical Strip Waveguide of Nanophotonics Lithium Niobate, *IEEE Photonics Journal*, 8(2), 7409919 (2016) [10.1109/JPHOT.2016.2531583](https://doi.org/10.1109/JPHOT.2016.2531583).
- [55] Abdul Muhsien M.; Salem E.T.; Agoool I.R., Preparation and characterization of (Au/n-Sn O<sub>2</sub> /Si O<sub>2</sub> /Si/Al) MIS device for optoelectronic application, *International Journal of Optics*, 2013, 756402 (2013) [10.1155/2013/756402](https://doi.org/10.1155/2013/756402).
- [56] Hattab, F. A., & Hamed, E. K. (2012). Laser Energy Effects on Optical Properties of Titanium Di-Oxide Prepared by Reactive Pulsed Laser Deposition. 30(1), 3104-3111.
- [57] Azzam Y. kudhur, Evan T. Salim, Ilker Kara, Rana O. Mahdi & Raed K. Ibrahim, The effect of laser energy on Cu<sub>2</sub>O nanoparticles formation by liquid-phase pulsed laser ablation, *J Opt* 53, 1309-1321 (2024). <https://doi.org/10.1007/s12596-023-01319-2>.
- [58] Jurn Y.N.; Malek F.; Mahmood S.A.; Liu W.-W.; Fakhri M.A.; Salih M.H., Modelling and simulation of rectangular bundle of single-walled carbon nanotubes for antenna applications *Key Engineering Materials*, 701, 57-66 (2016) [10.4028/www.scientific.net/KEM.701.57](https://doi.org/10.4028/www.scientific.net/KEM.701.57).
- [59] Fatema H. Rajab, Rana M. Taha, Aseel A. Hadi, Khawla S. Khashan & Rana O. Mahdi, Laser induced hydrothermal growth of ZnO rods for UV detector application, *Opt Quant Electron* 55, 208 (2023). <https://doi.org/10.1007/s11082-022-04473-2>.
- [60] Evan T. Salim, Rana O. Mahdi, Doaa Mahmoud, Subash C. B. Gopinath & Forat H. Alsultany, An Analysis Study Employing Laser Ablation in Gold Colloidal at Different Numbers of Laser Pulses, *Plasmonics* (2025). <https://doi.org/10.1007/s11468-025-02998-2>.
- [61] Tamara E Abdulrahman, Evan T Salim, Rana O Mahdi and MHA Wahid, Nb<sub>2</sub>O<sub>5</sub> nano and microspheres fabricated by laser ablation, *Advances in Natural Sciences: Nanoscience and Nanotechnology*, Volume 13, Number4, 045006 (2022), DOI [10.1088/2043-6262/ac99cf](https://doi.org/10.1088/2043-6262/ac99cf).
- [62] Khawla S. Khashan, Aseel A. Hadi, Rana O. Mahdi & Doaa S. Jubair, Aluminum-doped zinc oxide nanoparticles prepared via nanosecond Nd: YAG laser ablation in water: optoelectronic properties, *Opt Quant Electron* 56, 125 (2024). <https://doi.org/10.1007/s11082-023-05630-x>.
- [63] Hattab F.; Fakhry M., Optical and structure properties for nano titanium oxide thin film prepared by PLD, 2012 1st National Conference for Engineering Sciences, FNCES 2012, 6740474 (2012) [10.1109/NCES.2012.6740474](https://doi.org/10.1109/NCES.2012.6740474).